The International Archives of the Photogrammetry, Remote Sensing and Spatial Information Sciences, Volume XLVIII-1/W3-2023
2nd GEOBENCH Workshop on Evaluation and BENCHmarking of Sensors, Systems and GEOspatial Data
in Photogrammetry and Remote Sensing, 23–24 October 2023, Krakow, Poland

EVALUATION OF A GNSS/IMU/LIDAR-INTEGRATION FOR AIRBORNE LASER SCANNING USING RTKLIB PPK AND PPP GNSS SOLUTIONS

F. Pöppl[1]*, G. Mandlburger[1], N. Pfeifer[1]

[1]Technische Universität Wien, Vienna, Austria - (florian.poeppl, gottfried.mandlburger, norbert.pfeifer)@geo.tuwien.ac.at

KEY WORDS: Direct georeferencing, sensor orientation, sensor integration, trajectory estimation

ABSTRACT:

Airborne laser scanning allows for efficient acquisition of accurate 3D data for large areas. Because georeferencing of the LiDAR data requires knowledge of the platform trajectory, the laser scanner system commonly comprises a global navigation satellite system (GNSS) receiver/antenna and an inertial measurement unit (IMU). The standard processing pipeline consists of GNSS/IMU integration, georeferencing, and subsequent adjustment of the laser data. Here, we consider a holistic GNSS/IMU/LiDAR-integration approach based on least-squares adjustment. The GNSS is loosely coupled, and the GNSS positions are obtained using either post-processing kinematic or precise point positioning GNSS processing strategies using the open-source software RTKLib. In this contribution, we compare the resulting point clouds to those of a standard processing workflow and evaluate the impact of the different processing strategies on point cloud quality in terms of internal consistency and absolute accuracy for a airborne laser bathymetry (ALB) dataset. Although the GNSS solutions themselves differ strongly, both the PPK- and the PPP-derived point clouds show better strip differences (below 2.5 cm) and similar absolute accuracy (<4 cm RMSE w.r.t. reference targets after correction of constant datum shift) compared to the reference solution.

1. INTRODUCTION

Laser scanning is a widely used surveying technique based on light detection and ranging (LiDAR) in conjunction with a scanning mechanism. With the laser scanner mounted on a moving platform, large areas may be efficiently mapped and digitally represented as 3D point clouds. Here, we specifically consider airborne platforms. The laser scanner measurements consist of a range measurement together with one or two angular measurements. To transform the ranging and angle measurements of the laser scanner into a georeferenced coordinate system, the position and orientation of the scanner are required. Commonly, a global navigation satellite system (GNSS) receiver and antenna as well as an inertial measurement unit (IMU) are integrated with the laser scanner, which allows computing the required trajectory (Pöppl et al., 2023a).

The industry-standard approach is fusion of GNSS and IMU data using a Kalman filter, possibly followed by strip adjustment to reduce discrepancies between overlapping flight strips (e.g., Glira et al. 2015 and Jonassen et al. 2023). Various strategies exist for GNSS and IMU integration (Groves, 2013), most commonly: loose coupling (using pre-processed GNSS positions), tight coupling (using raw GNSS code and carrier phase measurements), or *deep* coupling (e.g., inertial aiding of GNSS tracking loop). While the tight coupling of GNSS and IMU is generally expected to be more accurate and robust compared to a standalone GNSS solution, a loose coupling of GNSS significantly reduces the complexity of the integration architecture and allows interchangeable use of different GNSS processing modes and software solutions. Strip adjustment, as an additional improvement of the trajectory subsequent to the GNSS/IMU integration, may be seen as loose coupling of LiDAR to the navigation sensors.

In this contribution, we consider a sensor fusion architecture based on loose coupling of GNSS and tight coupling of IMU and LiDAR. All measurements are considered simultaneously in a joint least-squares adjustment procedure (see Fig. 1), which is derived from the more general maximum a-posteriori (MAP) problem (Pöppl et al., 2023a). Similar methodology has already been applied in robotics applications (Cadena et al., 2016), photogrammetry (Cucci et al., 2017) and laser scanning (Brun et al., 2022). The advantage of tightly coupling IMU and LiDAR is the possibility of correcting short-term trajectory errors with less risk of deforming the point cloud than with classical strip adjustment which disregards the underlying navigation data.

In our recent work, we presented a GNSS/IMU/LiDAR-integration procedure for true direct georeferencing (i.e., without ground control) of airborne laser scanning data, together with possible ways of accounting for time-correlated GNSS errors in such a loose coupling (Pöppl et al., 2023b). We continue along the same line of investigation and evaluate (1) the use of loosely coupled GNSS in a joint GNSS/IMU/LiDAR-integration, (2) the suitability and accuracy of GNSS processing using the open-source RTKLib software in a high-end surveying application and (3) the differences between a differential post-processed kinematic (PPK) and a precise point positioning (PPP) solution.

This evaluation is performed for an airborne laser bathymetry (ALB) dataset acquired with a high-end laser scanner, and compares an industry-standard workflow with our GNSS/IMU/-LiDAR-integration, the latter processed separately with PPK- and with PPP-GNSS. Note that this is not a discussion of the technical details of PPK and PPP processing, but rather an attempt to analyze the the practical aspects of the RTKLib PPK- and PPP-solutions with respect to the GNSS solutions themselves, the estimated platform trajectory as well as the internal consistency and absolute accuracy of the final point cloud.

In Section 2, we describe the processing and evaluation methodology. In Section 3, we present the dataset used and evaluate the results, followed by a discussion and outlook in Section 4.

* Corresponding author

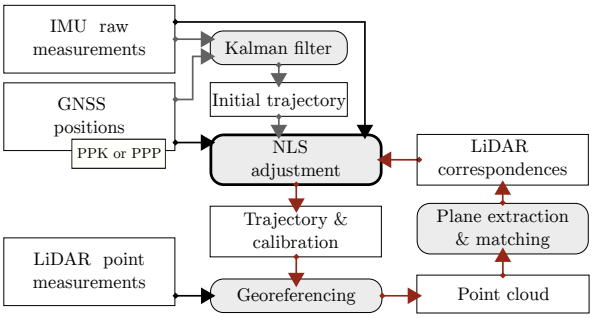

Figure 1. Processing workflow for the combined GNSS/IMU/LiDAR integration.

2. PROCESSING METHODOLOGY

The methodology for integrating the GNSS, IMU and LiDAR measurements is based on MAP estimation. Measurements $\boldsymbol{y}_i$, $i = 1, \ldots, n$ are modelled as explicit functions of the (unknown) parameters $\boldsymbol{x}$ plus noise

$$\boldsymbol{y}_i = f_i(\boldsymbol{x}) + \epsilon_i,$$

where the measurement errors ϵ_i are assumed to follow Gaussian distributions $N(\mathbf{0}, \boldsymbol{\Sigma}_i)$. Thus, the optimal (in the MAP sense) parameters are given by the non-linear least squares (NLS) estimator

$$\boldsymbol{x}^\star = \underset{\boldsymbol{x}}{\operatorname{argmin}} \sum_{i=1}^{n} (f_i(\boldsymbol{x}) - \boldsymbol{y}_i)^T \boldsymbol{\Sigma}_i^{-1} (f_i(\boldsymbol{x}) - \boldsymbol{y}_i). \quad (2.1)$$

In other words, the least-squares estimate $\boldsymbol{x}^\star$ minimizes the difference between model predictions $f_i(\boldsymbol{x})$ and measurements $\boldsymbol{y}_i$ for the GNSS, IMU and LiDAR measurements.

For the specific measurement equations as well as the modelling of time-correlated GNSS errors, refer to Pöppl et al. (2023a) and Pöppl et al. (2023b). The IMU measurements are used as output by the sensors, with no additional pre-processing. The LiDAR correspondences are derived from an initial georeferencing (cf. Fig. 1) using voxel-based plane extraction and matching. The GNSS measurement equations are adapted for use with a gyro stabilization mount by accounting for the GNSS antenna position, which varies with respect to the IMU coordinate system.

In a loosely coupled GNSS integration, the raw GNSS measurements are pre-processed and the derived antenna positions are included in the adjustment as observations. Here, we look at the suitability of using RTKLib for GNSS processing in the context of airborne laser scanning with high-end sensors. RTKLib (Takasu et al., 2009) is an open-source GNSS processing software capable of static and kinematic RTK, PPK and PPP processing. RTKLib is widely used in research, especially robotics (e.g., Li et al. 2020), but also integrated in commercial GNSS products such as *Emlid Studio* (Emlid, 2023). RTKLib is used here in two modes, PPK and PPP, to produce two different solutions. In both cases, all available constellations were used (GPS, Galileo, GLONASS, Beidou) together with final precise GNSS products and a 15 deg elevation mask. For the PPK processing, RTKLib's Kalman filter was run only in forward direction due to difficulties with ambiguity resolution in the combined forward-backward processing. For the PPP processing, the current RTKLib versions (2.4.2+) are capable of *unstable and experimental* ambiguity resolution (PPP-AR, Takasu 2013). Gurturk et al., 2022 investigated the accuracy of RTKLib's (among others) PPK and PPP with ambiguity resolution for two aircraft flights, with PPP-AR achieving a positioning accuracy of 6 cm compared to a PPK reference solution. However, we were unable to obtain any satisfactory results with RTKLib's PPP-AR and therefore use the *demo5* version (Everett, 2022b) where ambiguity resolution is disabled for PPP. The *demo5* version of RTKLib is primarily developed for low-cost receivers (Everett, 2022a), but has generally been more usable and reliable than the standard version in our testing. However, without ambiguity resolution, PPP is expected to be less accurate compared to the results from Gurturk et al. (2022). A generic antenna profile is available for the antenna, although use of this profile yielded no noticeable improvement - suggesting that the calibration may be inappropriate for this specific antenna unit or due to effects of the aircraft fuselage (cf. Rao 2013, Ch. 5).

The two resulting GNSS solutions are used separately as input in the adjustment procedure (Fig. 1) to obtain two trajectories. For each trajectory, an initial georeferencing is performed and the resulting point clouds are used (separately) for extracting and matching planar features. Then, the adjustments are repeated, now with GNSS, IMU *and* LiDAR measurements. The final trajectories and georeferenced point clouds are then evaluated.

3. DATA & RESULTS

The evaluation is carried out for a *RIEGL* VQ-880-GII airborne laser bathymetry (ALB) system, a high-end topo-bathymetric laser scanner integrated with an *Applanix* AP60 GNSS/IMU on a gyro stabilization mount. This ALB dataset was acquired in February 2023 in the area of the pre-Alpine Pielach river, near Loosdorf, Lower Austria (Fig. 2). In this area, high-quality reference data is available and will serve as ground truth for evaluating absolute accuracy. The reference data was acquired by RTK survey, with an expected accuracy of 1.5 cm in planimetry and 4 cm in altimetry[1].

Data from both the infrared and the green channel is included in all analyses. For the PPK processing, a virtual reference station (VRS) in the center of the study area is used due to the lack of close-by physical base station. In contrast, the advantage of PPP is of course the complete independence of any local infrastructure.

Fig. 3 shows the differences between the estimated GNSS antenna positions of the PPK- and PPP-solutions. The two solutions differ by up to 20 cm, especially for the height component. In addition to the time-varying discrepancies, a constant offset is present between both solutions (Table 1). After the adjustment process, the final trajectories are again compared (Fig. 4). The constant offset remains but the time-varying differences are reduced. Within the scan strips the discrepancies are reduced to below 2.5 cm due to the LiDAR-derived observations. Outside of the flight strips, i.e., when the airplane turns and no scan data is acquired, the differences largely remain (see Fig. 5 and Fig. 6). Note also that the difference becomes less noisy after adjustment due to the introduction of the (same) IMU measurements in both adjustments, which smooth out some of the higher-frequency components.

In Fig. 7, the final point clouds of three processing runs are compared: a) the proprietary workflow of tightly coupled GNSS/IMU processing using *Applanix*'s POSPac software, followed by strip adjustment using *RIEGL*'s RiPRECISION, b) our GNSS/IMU/-LiDAR-integration with the PPK-GNSS positions and c) our

[1] According to the RTK service provider.

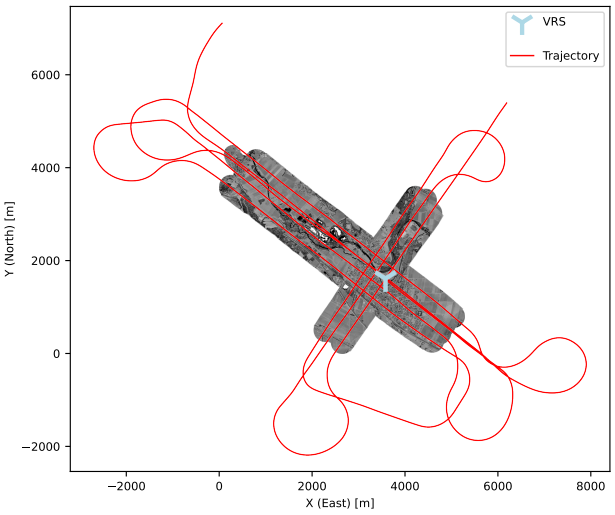

Figure 2. Platform trajectory and ALS point cloud colored by reflectance. Coordinates are given in a locally defined Cartesian coordinate system with east-north-up (ENU) axes.

	Shift x / y / z [cm]
GNSS (before adjustment)	-5.78 / 1.46 / -1.06
Trajectory (after adjustment)	-5.89 / 2.22 / -0.54

Table 1. Average difference between PPK- and PPP-solutions.

GNSS/IMU/LiDAR-integration with the PPP-GNSS positions. The strip differences are used as a measure of the internal consistency of the point cloud; here, the proposed adjustment method (both the PPK and the PPP variant) performs slightly better than the standard workflow, with strip differences reduced to below 2.5 cm (excepting vegetation). The distance to the reference data is determined by first selecting points within 1 m of the reference target, then estimating a best-fitting plane and computing the normal distance from the reference target's position to the plane. In terms of absolute accuracy, all three solutions exhibit a (different) datum shift with respect to the reference targets. Because the reference targets are made up of horizontal ground control points and sloped rooftops of varying azimuth, the 3-parameter (X/Y/Z) datum shift may be recovered by minimizing the root mean squared error (RMSE) of normal distance between point cloud and ground truth (i.e., by linear least-squares). Table 2 shows the estimated datum shifts for all three solutions, as well as the RMSE after application of the datum shift. The datum shifts are different, but of similar magnitude (∼10 cm) and the RMSE (after shifting) for all solutions is below 4 cm. Note that while the PPK- and PPP-GNSS solutions initially show time-varying differences of up to 20 cm to

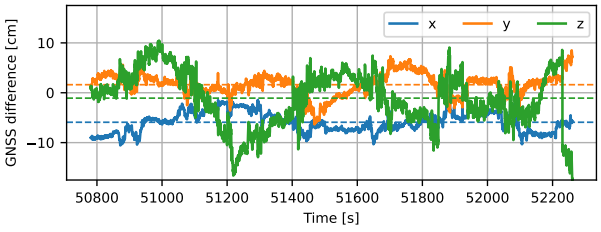

Figure 3. Differences in position between the PPK- and the PPP-processed GNSS solution, over time. The mean differences (cf. Table 1) are shown as dashed lines.

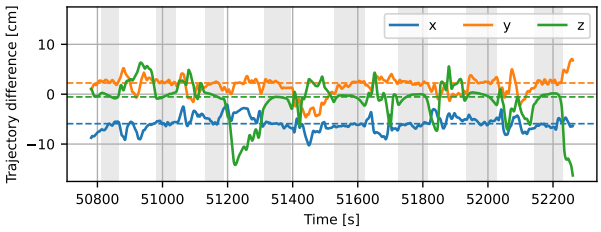

Figure 4. Differences in position between the final trajectories after adjustment using PPK-GNSS and after adjustment using PPP-GNSS, over time. Time periods marked in gray correspond to the flight strips (i.e., where LiDAR data is acquired). The mean differences (cf. Table 1) are shown as dashed lines.

	Shift x / y / z [cm]	RMSE [cm]
Proprietary	-3.32 / 5.26 / -6.82	3.98
PPK-adjustment	0.74 / 8.93 / 1.76	3.76
PPP-adjustment	-5.10 / 11.46 / 1.31	3.74

Table 2. Datum shift and RMSE for all three solutions, derived by fitting the point clouds to the reference targets. Note that the point cloud shifts for the PPK- and the PPP-adjustment differ by -5.85 / 2.53 / -0.44 , which matches the average difference between the trajectories in Table 1.

each other, this reduces to a maximum difference of 2.5 cm after adjustment for both trajectory and point cloud. Unsurprisingly, the initial constant difference in the GNSS positions (Table 1) carries over to the datum shift (Table 2). This implies that while short-term errors can be corrected by inclusion of the LiDAR data, long-term effects (including constant shifts) cannot.

The height difference between the PPK and the PPP blocks are shown in Fig. 8, and are below 2.5 cm. The block differences correlate highly with the position differences of the adjusted trajectory, with the larger differences in the locations where the trajectory solutions show a corresponding difference in position (see Fig. 6). A closer look at the area marked with the black rectangle in Fig. 8, where the block difference reaches 2 cm and suitable reference targets are available, confirms a positional shift affecting the whole area which is also reflected in the reference target distances (see Fig. 9). Specifically, the locations of all ground control points, as determined from the respective point clouds, are shifted in height by 1-1.5 cm. Conversely in the area of negative block difference, the ground control points are shifted in the other direction. Therefore, it is unclear which solution is superior as both strip differences and RMSE w.r.t. reference are the same for PPK and PPP. But, both show similar or better point cloud quality than the proprietary solution.

The constant datum shift between the PPK-solution and the reference data may have different reasons. It is possible that GNSS processing errors, such as insufficient treatment of atmospheric effects, may account for some of it. Since different base stations were used for the acquisition of the reference data (using RTK-GNSS) and the kinematic processing (PPK), a possible datum error somewhere along the processing chain cannot be fully excluded. The RMSE after application of the datum shift is in line with the expectations for the accuracy of the reference data, but the constant offset is likely systematic. Still, this is not limited to the RTKLib processing, as a different constant offset of similar magnitude was determined when processing with the industry-standard proprietary workflows of the navigation system and laser scanner manufacturers.

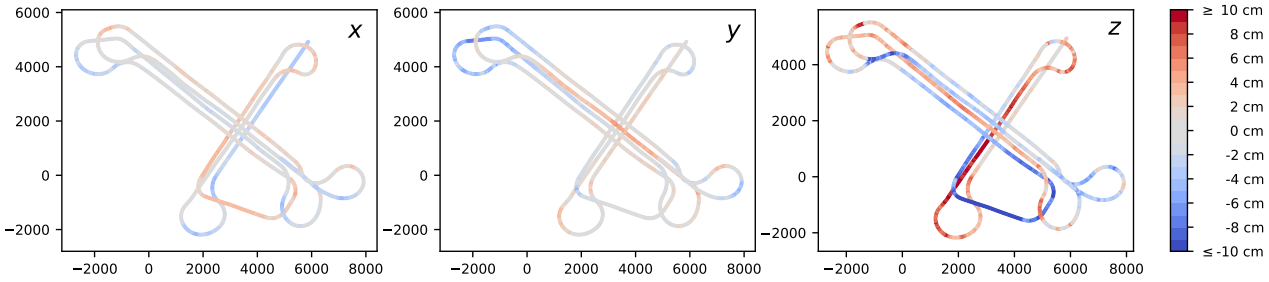

Figure 5. De-meaned differences in position between the PPK- and the PPP-processed GNSS solution for X, Y and Z axes (ENU).

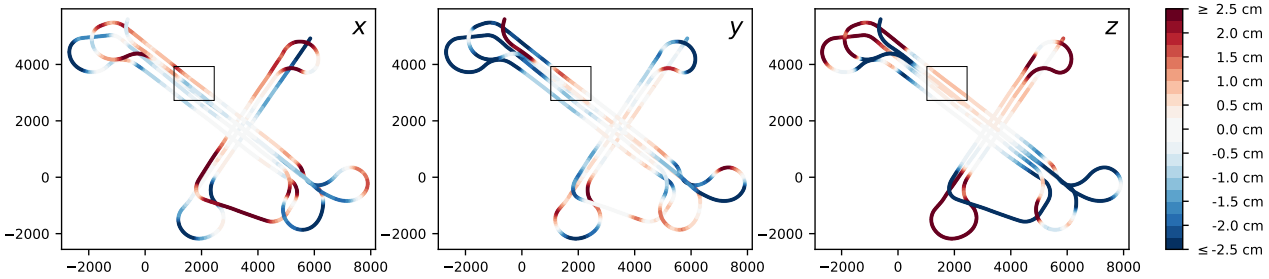

Figure 6. De-meaned differences in position between the trajectory obtained from the PPK-GNSS/IMU/LiDAR adjustment and the trajectory obtained from the PPP-GNSS/IMU/LiDAR adjustment, for X, Y and Z axes (ENU). In comparison to Fig. 5, this depicts the remaining time-varying differences in platform position after exploiting the overlaps in the LiDAR data to correct trajectory errors.

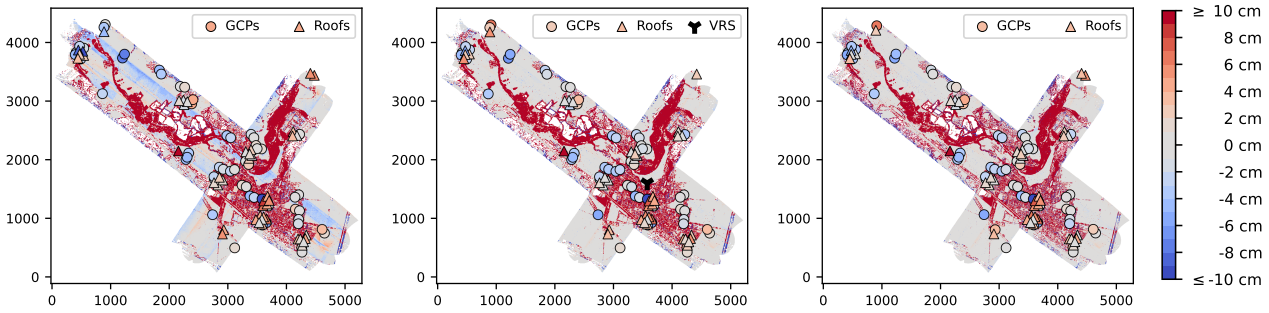

(a) Proprietary solution. (b) PPK-based solution. (c) PPP-based solution.

Figure 7. Maximum pairwise height differences of all strips and normal distances to reference targets. The 98 reference targets are made up of approximately 55 horizontal ground control points and 43 sloped rooftops. Their coordinates are shifted slightly for better visualization.

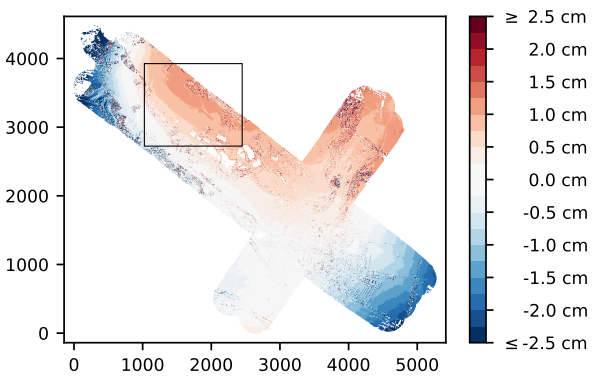

Figure 8. Difference in average height between the point cloud resulting from the PPK-GNSS/IMU/LiDAR adjustment and the point cloud resulting from the PPP-GNSS/IMU/LiDAR adjustment. The black rectangle marks the area shown in Fig. 9.

4. DISCUSSION

In summary, the results using RTKLib, and especially the negligible difference between PPP- and PPK-derived point clouds, are promising. The final point cloud obtained using the GNSS/-IMU/LiDAR-integrated georeferencing approach together with open-source RTKLib-based GNSS processing proves to be comparable in quality to the results of an industry-standard workflow of GNSS/IMU integration followed by strip adjustment. With respect to loose coupling of the GNSS measurements, we conclude that (1) constant or long-term shifts intrinsically cannot be eliminated by such an adjustment and (2) time-varying errors are correctable if sufficient redundant information from overlapping LiDAR strips is present. The tight-coupling of IMU and LiDAR helps to avoid block deformations, which may occur in control-free strip adjustment. More analysis is needed to determine the minimum amount of overlap and optimal flight patterns to guarantee sufficient correction of the GNSS errors. If time-varying errors can be eliminated and only a constant datum shift is present, this could be rectified by introducing control points as usual, but requiring a much lower number of control points as might otherwise be necessary.

While the results are encouraging, the RTKLib software is somewhat restricted in terms of usability (parametrization of the algorithms, restrictions on input data formats, possibility to use certain precise GNSS products for PPP). Additionally, RTKLib is not yet capable of resolving ambiguities reliably and consistently in PPP, and may also have difficulties with PPK ambiguity resolution in airborne scenarios with longer baselines. Should this be fixed, further improvements in the direct georeferencing accuracy may be expected in the future. The block difference between the PPK-derived point cloud and the PPP-derived point cloud strongly imply a systematic effect, but the difference cannot be explained by a datum shift. A larger study area, together with dense ground truth data, would help further investigation.

However, such data is not yet (publicly) available as data acquisition requires significant time and effort, especially for the large spatial scale of representative airborne laser scanning data acquisitions. When acquiring reference data for the purposes of benchmarking different georeferencing methods, special care must be taken to ensure the accuracy of the reference data is sufficiently high, which is challenging considering the errors are at the centimeter-level. In data acquisitions involving multiple measurement methodologies, and carried out by multiple parties, one must ensure the use of a single consistent datum for all acquired data. Even then, no fully standardized methods have been established to date for comparison of trajectories and point clouds. Introduction of suitable benchmark data together with standardized methods for evaluation will enable the development of more accurate and more efficient georeferencing methods in the future.

ACKNOWLEDGMENTS

This work was carried out as part of the project ZAP-ALS (883660) funded by the Austrian Research Promotion Agency (FFG[2]).

REFERENCES

Brun, A., Cucci, D. A. and Skaloud, J. (2022). 'LiDAR Point–to–Point Correspondences for Rigorous Registration of Kinematic Scanning in Dynamic Networks'. In: *ISPRS Journal of Photogrammetry and Remote Sensing* 189, pp. 185–200. DOI: 10.1016/j.isprsjprs.2022.04.027.

Cadena, C., Carlone, L., Carrillo, H., Latif, Y., Scaramuzza, D., Neira, J., Reid, I. and Leonard, J. J. (2016). 'Past, Present, and Future of Simultaneous Localization And Mapping: Towards the Robust-Perception Age'. In: *IEEE Transactions on Robotics* 32.6, pp. 1309–1332. DOI: 10.1109/TRO.2016.2624754.

Cucci, D. A., Rehak, M. and Skaloud, J. (2017). 'Bundle Adjustment with Raw Inertial Observations in UAV Applications'. In: *ISPRS Journal of Photogrammetry and Remote Sensing* 130, pp. 1–12. ISSN: 09242716. DOI: 10.1016/j.isprsjprs.2017.05.008.

Emlid (2023). *Emlid Studio User Documentation*. URL: https://emlid.com/wp-content/uploads/2023/06/Emlid_Studio_User_Documentation.pdf (visited on 30/06/2023).

Everett, T. (2022a). '3rd Place Winner: 2022 Smartphone Decimeter Challenge: An RTKLIB Open-Source Based Solution'. In: 35th International Technical Meeting of the Satellite Division of The Institute of Navigation (ION GNSS+ 2022). Denver, Colorado, pp. 2265–2275. DOI: 10.33012/2022.18376.

Everett, T. (2022b). *RTKLib Demo5*. Version 2.4.3 b35g. URL: https://github.com/rtklibexplorer/RTKLIB (visited on 30/06/2023).

Glira, P., Pfeifer, N., Briese, C. and Ressl, C. (2015). 'Rigorous Strip Adjustment of Airborne Laserscanning Data Based on the ICP Algorithm'. In: *ISPRS Annals of Photogrammetry, Remote Sensing and Spatial Information Sciences* II-3/W5, pp. 73–80. DOI: 10.5194/isprsannals-II-3-W5-73-2015.

Groves, P. D. (2013). *Principles of GNSS, Inertial, and Multisensor Integrated Navigation Systems*. 2nd ed. GNSS Technology and Application Series. Boston: Artech House. 776 pp. ISBN: 978-1-60807-005-3.

Gurturk, M. and Soycan, M. (2022). 'Accuracy Assessment of Kinematic PPP Versus PPK for GNSS Flights Data Processing'. In: *Survey Review* 54.382, pp. 48–56. ISSN: 0039-6265, 1752-2706. DOI: 10.1080/00396265.2020.1865016.

Jonassen, V. O., Kjørsvik, N. S. and Gjevestad, J. G. O. (2023). 'Scalable Hybrid Adjustment of Images and LiDAR Point Clouds'. In: *ISPRS Journal of Photogrammetry and Remote Sensing* 202, pp. 652–662. DOI: 10.1016/j.isprsjprs.2023.07.007.

Li, T., Pei, L., Xiang, Y., Wu, Q., Xia, S., Tao, L. and Yu, W. (2020). 'P3-LOAM: PPP/LiDAR Loosely Coupled SLAM with Accurate Covariance Estimation and Robust RAIM in Urban Canyon Environment'. In: *IEEE Sensors Journal*. DOI: 10.1109/JSEN.2020.3042968.

[2] Österreichische Forschungsförderungsgesellschaft, Vienna, Austria, www.ffg.at

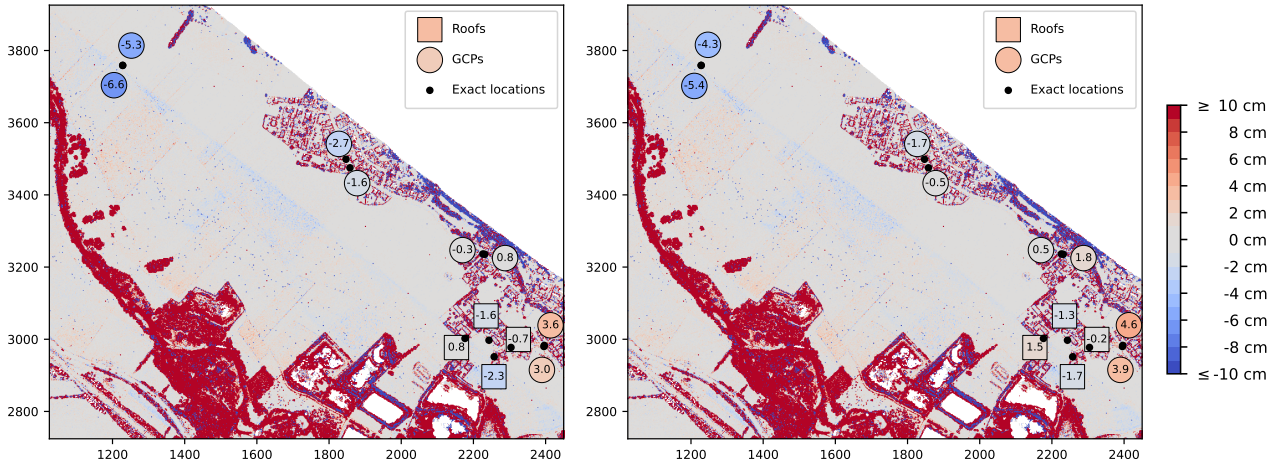

(a) PPK-based point cloud.

(b) PPP-based point cloud.

Figure 9. Strip differences and distances to reference targets of sub-area with high block differences, area marked in Fig. 8.

Pöppl, F., Neuner, H., Mandlburger, G. and Pfeifer, N. (2023a). 'Integrated Trajectory Estimation for 3D Kinematic Mapping with GNSS, INS and Imaging Sensors: A Framework and Review'. In: *ISPRS Journal of Photogrammetry and Remote Sensing* 196, pp. 287–305. ISSN: 09242716. DOI: 10.1016/j.isprsjprs.2022.12.022.

Pöppl, F., Pfennigbauer, M., Ullrich, A., Mandlburger, G., Neuner, H. and Pfeifer, N. (2023b). 'Modelling of GNSS Positioning Errors in a GNSS/INS/LiDAR-integrated Georeferencing'. In: *Publikationen Der Deutschen Gesellschaft Für Photogrammetrie, Fernerkundung Und Geoinformation e.V.* 3. Wissenschaftlich-Technische Jahrestagung Der DGPF, pp. 183–196.

Rao, B. R., ed. (2013). *GPS/GNSS Antennas*. GNSS Technology and Applications Series. Boston: Artech House. 404 pp. ISBN: 978-1-59693-150-3.

Takasu, T. (2013). *RTKLIB Ver. 2.4.2 Manual*. URL: http://www.rtklib.com/prog/manual_2.4.2.pdf (visited on 28/08/2023).

Takasu, T. and Yasuda, A. (2009). 'Development of the Low-Cost RTK-GPS Receiver with an Open Source Program Package RTKLIB'. In: *International Symposium on GPS/GNSS*. Jeju, Korea, p. 7.